 MCB, vol.1, no.2, pp.123-131, 2004

Understanding Actin Organization in Cell Structure through Lattice Based Monte Carlo Simulations

Kathleen Puskar[1], Leonard Apeltsin[2], Shlomo Ta'asan[3], Russell Schwartz[2], Philip R. LeDuc[4]

Abstract: Understanding the connection between mechanics and cell structure requires the exploration of the key molecular constituents responsible for cell shape and motility. One of these molecular bridges is the cytoskeleton, which is involved with intracellular organization and mechanotransduction. In order to examine the structure in cells, we have developed a computational technique that is able to probe the self-assembly of actin filaments through a lattice based Monte Carlo method. We have modeled the polymerization of these filaments based upon the interactions of globular actin through a probabilistic model encompassing both inert and active proteins. The results show similar response to classic ordinary differential equations at low molecular concentrations, but a bi-phasic divergence at realistic concentrations for living mammalian cells. Further, by introducing localized mobility parameters, we are able to simulate molecular gradients that are observed in non-homogeneous protein distributions *in vivo*. The method and results have potential applications in cell and molecular biology as well as self-assembly for organic and inorganic systems.

1 Introduction

The ability of a cell to sense and respond to mechanics is important due to the diversity of associated abnormal maladaptive responses, which include coronary heart disease and congestive heart failure (Jensen et al, 1994; Kiss et al, 1995; Takeishi et al, 2001). Research in the field of mechanotransduction has explored the link between mechanical stimulation and biochemical signaling through molecular mechanisms including ion channels and molecular conformational changes(Sachs, 1991; Wang et al, 1993; Yamazaki et al, 1998; LeDuc et al, 1999). Research into signaling responses has provided insight into the regulation of the mitogen-activated protein kinase pathways including p38 and Jun, showing identifiable changes in gene expression profiles in response to mechanical stimulation (Resnick et al, 1997; Li et al, 1999; Meyer et al, 2000; Ferrer et al, 2001). While the precise mechanism for this cascade has not been determined, it is well known that the cytoskeleton plays an essential role in this process. The actin cytoskeleton is linked from the extracellular into the intracellular environment through a series of proteins forming a mature heterocomplex called the focal adhesion complex (FAC). The FAC is comprised of proteins including transmembrane integrins, vinculin, paxillin, and talin (Wang et al, 1993; Moulder et al, 1996; Tang et al, 2002). As the integrins bind to the extracellular matrix, a physical connection is extended through the cell membrane. The cytoskeleton has also been implicated influencing a variety of cellular processes including cell motility where there is a significant increase in actin polymerization at the leading edge of chemotactic cells (Valerius et al, 1982; Hodgson et al, 2000; Chen et al, 2003). Also, during cell division, the microtubule and actin organization is important in the formation of the mitotic spindle for chromosome division and pinching of the cell in cytokinesis (White et al, 1981; Alfa et al, 1990; Rao et al, 1990; Schaerer-Brodbeck et al, 2000). To probe the cytoskeleton and its effects on the mechanochemical signaling, understanding the assembly of these spatiotemporally variable systems is requisite in the biological realm.

As our knowledge of biological systems becomes more intricate, computational modeling efforts are becoming essential in understanding the implications of low-level manipulations across whole systems. Probing the mechanical behavior of the cytoskeleton and its interaction with diverse intracellular systems will require the amalgamation of novel computational methods integrated

[1] Department of Mechanical Engineering
[2] Biological Sciences and Computer Science, and
[3] Mathematical Science, Carnegie Mellon University, 5000 Forbes Avenue, Pittsburgh, Pennsylvania 15213
[4] Corresponding Author: Department of Mechanical Engineering, Carnegie Mellon University, 5000 Forbes Avenue, 415 Scaife Hall, Pittsburgh, Pennsylvania 15213, (e-mail: prleduc@cmu.edu)

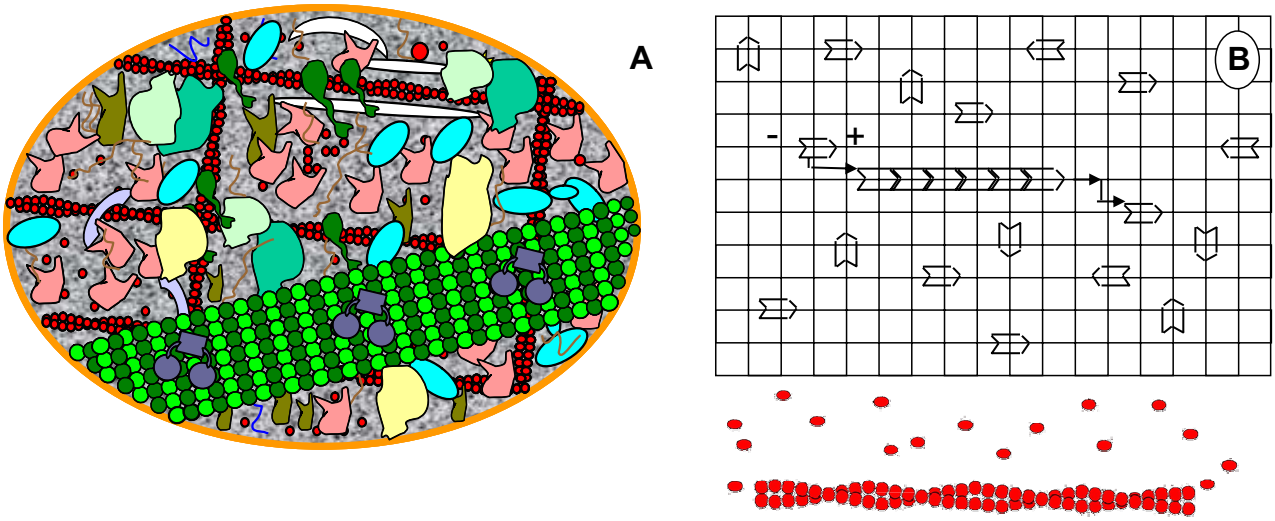

Figure 1 : The crowded cellular environment and LaBB (Lattice Based Biological Monte Carlo) modeling system. (A) Drawing of the crowded molecular environment for *in vivo* cellular conditions (B) Schematic of the LaBB model depicting globular actin (G-actin) binding and linear filament polymerization on a square lattice grid.

with experimental results in a more inclusive setting. As with any highly complex system, though, identifying the relevant constituents is essential to building efficient models while generating meaningful data. This requires characterizing the input of the pertinent subsystems in the context of a larger venue. Current systems biology approaches to modeling cellular biochemistry require many abstractions. One critical generalization that is conventionally employed is removing spatial considerations. Classical methods assume that biochemical reactions transpire in a large, homogeneous, uncrowded environment; the individual reactants can combine and diffuse together without steric hindrance from molecules uninvolved with a given reaction (Gamble et al, 1987; Hernandez-Cruz et al, 1990; Goodsell, 1993). These models are parameterized for kinetic rate constants generally derived experimentally *in vitro* under conditions closely matching those assumed by the models. This strategy, while convenient, is not an accurate depiction for a cell or sub-cellular compartment (Fig. 1A), in which closely packed molecules, abrupt local concentration gradients, minimal individual subunits, and irregularly shaped or small compartments create deviations from the ideal environment assumed by the classical simulations (Minton, 2001; Hall, 2002; Marx, 2003).

We developed the LaBB (Lattice Based Biological Monte Carlo) model to examine spatial considerations on cellular biochemistry. We specifically implement a simplified model of assembly and disassembly for actin filaments. We mathematically model the one-dimensional constrained formation of actin filaments from globular actin (G-actin) to study the kinetics and thermodynamics of actin polymerization and depolymerization. These properties are examined as functions of actin monomer and inert particle concentrations as well as induced molecular gradients indicative of directed motility. Space-aware modeling methods are compared to a space-free simulation method using classical ordinary differential equations (ODEs) where kinetic rates have been well established in order to determine conditions under which spatial factors produce measurable effects on cellular biochemistry. Here we examine a defined one-dimensional constrained system in biological filament assembly in order to understand their behavior in the physiological milieu.

2 Methods

We implement a probabilistic coarse-grained variant of cellular automaton, LaBB, to account for spatial influences on macromolecular assembly systems. This describes a system as a grid of discrete spatial units, each with a discrete state as well as rules governing how the unit state can transform over time with relation to the attributes of the adjoining sites. These coarse-grained

models utilizing small parameter spaces are effective for probing how high-level system properties can develop from low-level physical relationships for determining emergent properties for system response (Henson et al, 2001; Levine et al, 2001; Shabunin et al, 2002). LaBB is a special instance of the generalized class of Monte Carlo models, where a system transitions among an array of discrete states with respect to a defined set of probabilities (Puskar et al, 2004).

Actin organizes itself into filaments from an initial monomeric form and is polarized with two structurally different ends. The LaBB model represents actin monomers as discrete units which move according to a Brownian motion model with periodic boundary conditions along a rectangular lattice (Fig. 1B). Inert particles can either move or remain stationary depending upon the boundary conditions imposed upon them. Initially, monomers and inert particles are placed randomly on the lattice. The monomers have one of four orientations and with each time step all unbounded monomer states are updated. Their movement is based upon a probability for occupying the four adjacent positions or remaining in the same lattice position. A monomer cannot move into an already occupied adjacent site, and thus particles occupying these bordering positions increase the probability for a non-mobile response. A binding interaction potentially proceeds when a filament end is adjacent to a monomer or two free monomers are in adjoining sites with the proper orientation. Once bound, actin is not allowed to change location or orientation. The model also incorporates a probability of shedding monomers from the ends of actin filaments, similar to the disassociation rate for non-spatial models. The assembly of linear molecular filaments has its genesis as an initial distributed monomer form proceeding to filaments, which results in a pseudo steady-state response. Lattice density, orientation, spatial location, and binding and unbinding probabilities collectively represent both entropic and enthalpic components of binding that would be captured by association and dissociation rates in a non-spatial representation or by those rates in a diffusion-reaction model.

Both actin and non-reactant particles correspond to mutually impenetrable sites affecting molecular mobility. In a crowded environment the effect of specie concentrations on polymerization should be discernible through binding rates and filament length distributions. To study this effect, LaBB model simulations are performed separately over a range of actin and inert particle concentrations. Concentrations are based on the total monomer and/or inert particles per volume; this is calculated assuming a unit grid spacing of 10 nanometers and a normalized depth of 10 nanometers. The definitions for the binding rates are derived directly from the numerical formulation of the ODE model for this system, and grid volumes normalize the rates between spatially different models. The LaBB model separately tracks the changes in free monomer and filament quantities; the rate constants are calculated using the numerical approximations described in equation 1.

$$k_+ = \left[\frac{a_1(t+\Delta t)-a_1(t)}{\Delta t}\right] \times \left(a_1(t)\sum_{j=1}^{N} a_j(t)\right) \times Volume$$
$$k_- = \left[\frac{a_1(t+\Delta t)-a_1(t)}{\Delta t}\right] \times \left(a_2(t)+\sum_{j=2}^{N} a_j(t)\right) \times Volume \quad (1)$$

Each rate constant is estimated by averaging over five simulations of 50,000 time steps. This allows comparison of the LaBB model, where the rate constant is potentially a function of spatial factors, to traditional ODE models, where the rate constant is a parameter of the system presumed independent of solution concentration.

We first study the effect of crowding on molecular polymerization by varying actin quantities between 100 and 5,000 monomers without inert particles, maintaining a constant grid space of 100 by 100 lattice sites; this equates to pure actin concentrations of 16.6μM to 830 μM. We examine the influence of nonparticipating molecules on these reactions by introducing stationary, inert particles in quantities of 0 to 6,000 while maintaining a constant of 1000 monomers and a grid space of 100 by 100 lattice sites. Simulations for a range of grid space reveal no noticeable grid size effects on binding rates. Finally we bias the mobility probabilities in the LaBB model to influence molecular migration to localized areas. We finally examine these effects in a model of extended cellular space. All simulations are initialized with random distributions of particles across the space.

3 Results and Discussion

The organization of the actin assembly is modeled based upon molecular interactions of G-actin monomers and non-binding inert particles. Snapshots taken during these

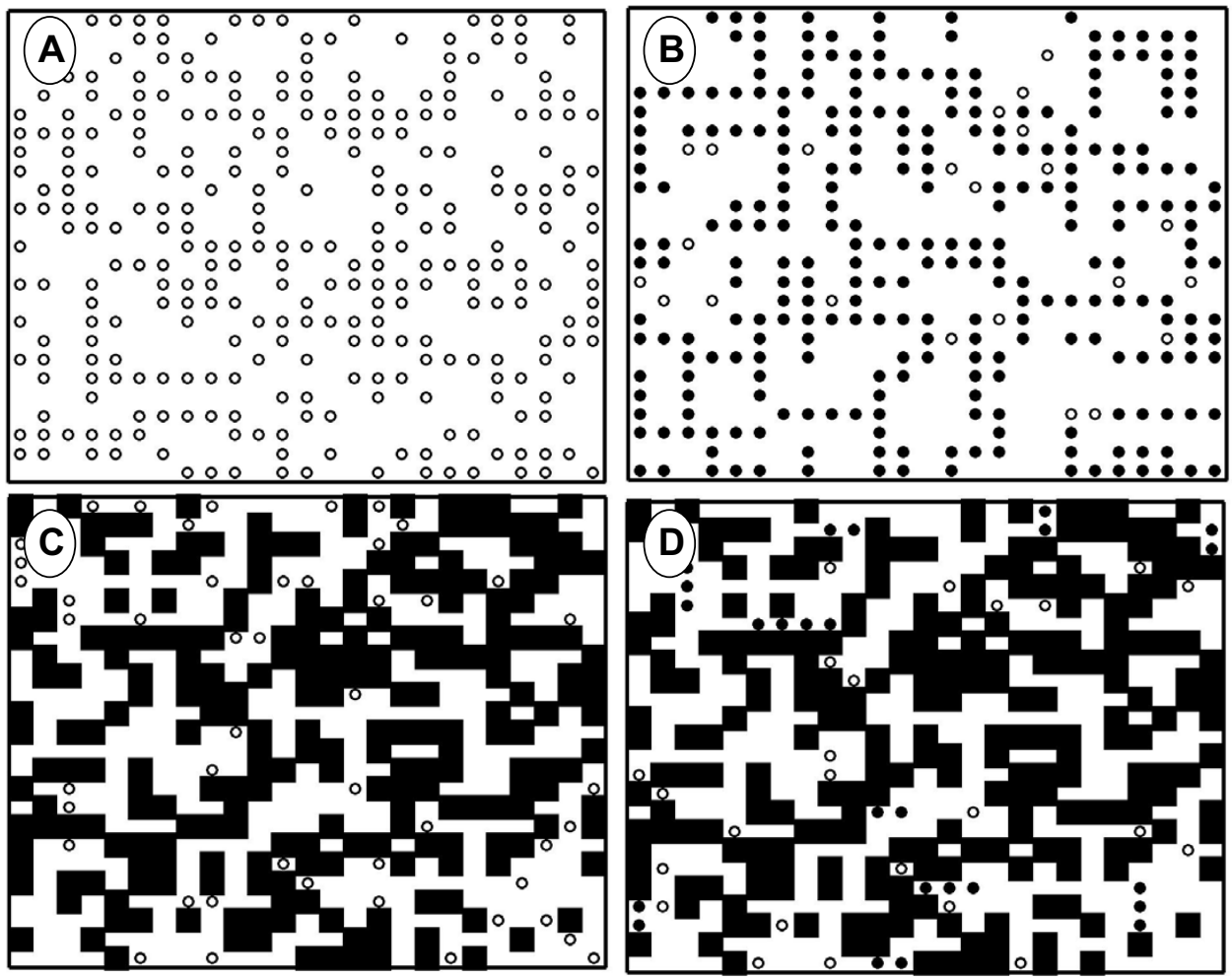

Figure 2 : Snapshots of actin polymerization models with G-actin monomers, actin filaments, and inert particles. (A) Simulation of actin polymerization at time zero for a high concentration of free G-actin (open circles) at 830 μM. (B) Simulation at a pseudo-steady state with polymerized filaments (solid circles) and free G-actin monomers. (C) Initial distribution for 830 μM of total particle concentration with 166 μM of free G-actin monomers and 664 μM of inert particles (solid squares). (D) Simulation at a pseudo-steady state with the protein concentrations from (C). All simulations are 100 by 100 grid spacing with probabilities of polymerization of 1.0 and dissociation of 0.01.

simulations with and without inert particles indicate how crowded molecular environments can affect polymerization. In the absence of inert particles, actin monomers initially have relatively unrestricted interactions (Fig. 2A). As binding and diffusion occurs, nucleated filaments evolve through 2 monomers binding together. This affects the polymerization due to the growth of filaments and movement of monomers through the exclusionary site constraint. At a higher concentration the interference between polymerized and individual monomers increases, which amplifies their potential to occupy adjacent sites and thus enhances the polymerization process (Fig. 2B). Conversely, when inert particles are introduced, they form obstacles in the diffusion paths of actin monomers (Fig. 2C). As the concentration of inert particles increases, a greater number of sites surrounding the monomers and filaments are occupied by these particles. Therefore, the binding sites available for filament growth are limited by inert monomer interference, which decreases the meeting potential, inhibiting polymerization (Fig. 2D).

The binding rates extracted from the LaBB model for the pure actin concentrations, and also the combined inert

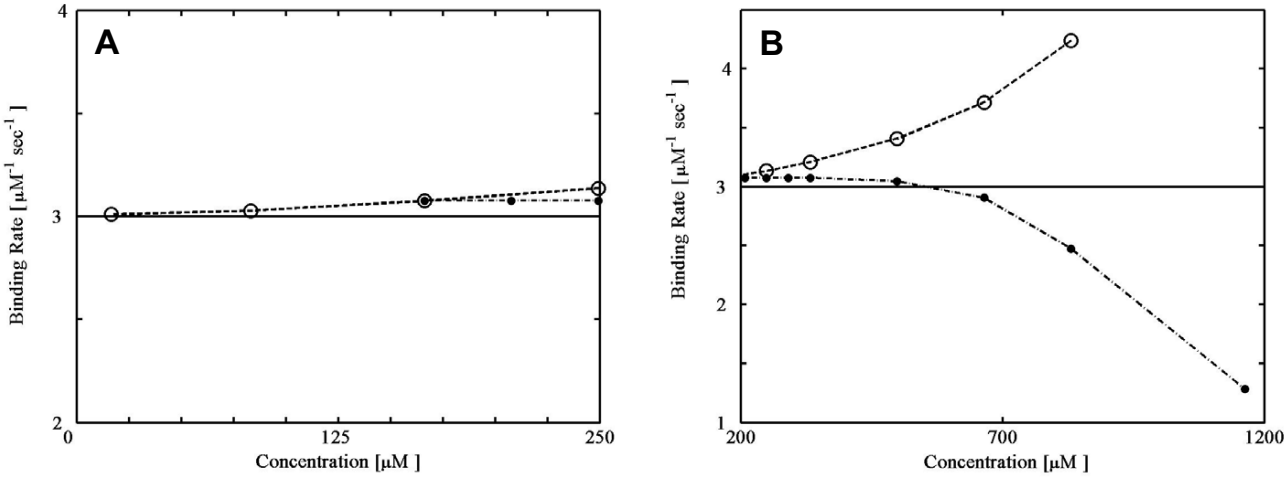

Figure 3 : Binding rate constants for LaBB and ODE (Ordinary Differential Equation) models. (A) Binding rate constants for the ODE model (solid line) and the LaBB model (open circle) for pure actin, and actin-inert particle scenario (solid circle) for lower concentrations typical of *in vitro* conditions. (B) Divergence of binding rate constants for the ODE and LaBB models at higher *in vivo* concentrations indicative of molecular crowding in cells. The error bars are omitted for clarity; a standard deviation of 1% or less is typical, with a peak value of 5% for the 830 μM actin-inert particle data.

particle and actin concentrations reveal unique responses. Since the ODE model does not account for concentration effects, the binding rate is depicted at a constant value over the entire range. This is derived from the LaBB model at a low, pure monomer concentration of 16.6 μM ($<$ 1mg/mL) typical of *in vitro* conditions and consistent with the inherent assumptions of the ODE. At these low levels the estimated binding rates from the LaBB model are nearly independent of concentration (Fig. 3A) and exhibit virtually identical results to the ODE. But as concentration increases, the model diverges from the ODE solutions for both the pure monomer and the combined monomer-inert particle scenarios (Fig. 3B). For pure actin levels of 166 μM and above spatial effects begin to influence binding rates significantly. At 400 μM, the estimated binding rate from the LaBB model is 24% greater than the apparent rate constant extracted at low concentrations; 350 μM of total actin is not uncommon in cells (Alberts et al, 1994). Rate constants for the inert particle simulations appear unaffected until total concentrations above 500 μM are reached. At 1.2 mM the binding rate decreases 58% from the estimated value for the same actin population without inert particles present (Fig. 3B); total molecule concentrations from 0.8 to 8 mM are revealed in macromolecular crowding *in vivo* (Minton, 2001).

The simulation reveals that with an increase in G-actin proteins into the model, the effective polymerization rate constant increases significantly. In cell motility, a rapid increase in the polymerization process occurs at the leading edge of cells, which is associated with an amplification of the individual monomer concentrations. Conversely, when the additional proteins in the simulation are inert and thus have no ability to bind to the self-organizing structures, the polymerization is slowed. Further, filament length distributions also differ at higher concentrations. For 830 μM monomer concentration, the ODE and LaBB distributions are markedly different, with an increase in the number of longer filaments in the LaBB simulation. With inert particles at 830 μM the filament length distributions resulting from the LaBB simulations diverge from the ODE distributions as the number of longer filaments decreases (data not shown). The effect of these changes on filament length distributions suggests that they are likely to significantly impact even gross morphological and mechanical properties of cell structure models.

These results have important implications for the modeling of cellular systems. The LaBB model shows significant deviations from constant reaction rates in the presence of either high reactant concentration or high concentration of an inert molecule that would not conven-

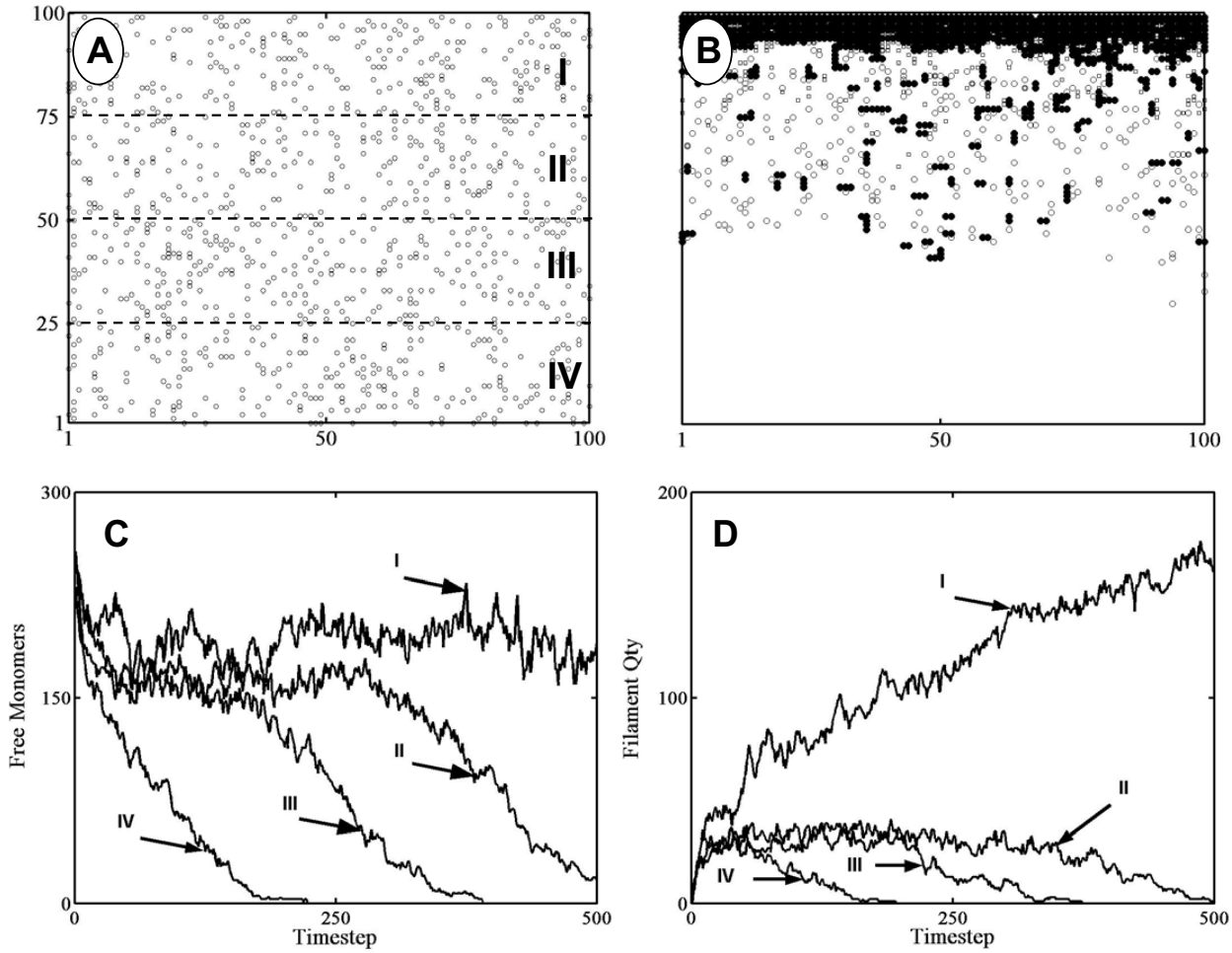

Figure 4 : Snapshots and actin distribution in polarized filament formation. (A) Initial random distribution of 1000 monomers (open circles) on a 100 by 100 lattice. The entire lattice is divided equally into four quadrants (I, II, III, IV) of 25 by 100 sites distributed across the ordinate. (B) Distribution of actin monomers and filaments (solid circles) at 500 time steps with a probability of 2:1 for moving vertically toward quadrant I. (C) Monomers and (D) total filaments present in each quadrant as a function of time.

tionally be considered a reactant in the polymerization reaction. Neither of these effects would appear in a traditional space-free ODE model or even a space-aware reaction-diffusion model. The LaBB model converges with the ODE model in low concentration domains typical of *in vitro* biochemistry conditions under which simulation parameters would traditionally be derived. Total molecular concentrations in cellular environments can be around the order of 50-400 mg/mL (Minton, 2001; Marx, 2003). In these biologically-relevant high-concentration domains, traditional models parameterized from low-concentration *in vitro* simulations would yield markedly different estimates of true reaction rates than a LaBB model that accounts for steric hindrance and excluded volume effects at physiological concentrations.

Another aspect of cellular biochemistry that may be inadequately accounted for in prior models is the highly non-uniform distribution of reactants in the cell. For example in actin polymerization during cell motility, a gradient of monomer concentrations is observed with a significantly higher density at the leading edge. We model this gradient by introducing a transport mechanism for the actin to simulate the polarized distribution of monomer concentration toward the leading edge of a cell during chemotaxis. Initially there is a uniform distribution of the actin monomers in the simulation space (Fig. 4A). The bias is

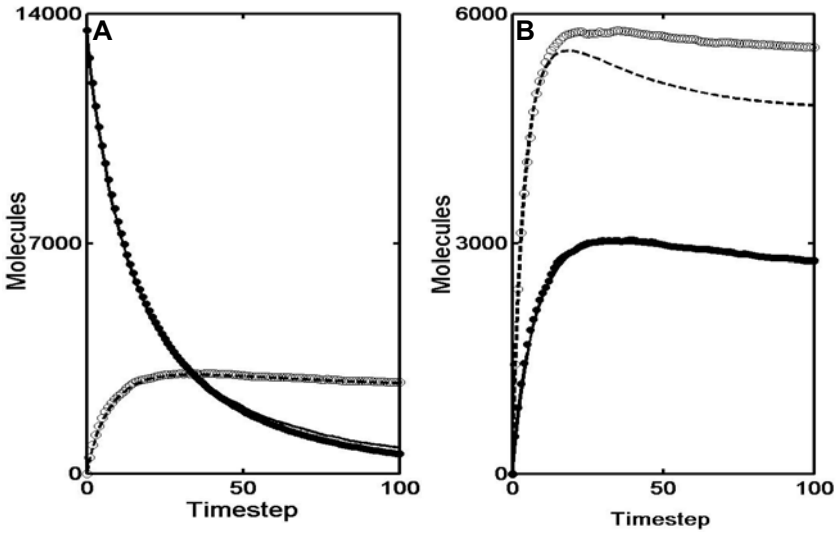

Figure 5 : Actin binding in a three dimensional LaBB and space-free ODE model. (A) Distributions of monomers and dimers versus time for ODE and LaBB models from initial monomer concentrations of 830 μM. The figure shows ODE monomer (solid line), ODE dimer (dashed line), LaBB monomer (solid circles), and LaBB dimer (open circles) concentrations as a function of time. (B) Distribution of dimers versus time step for ODE and LaBB models at 830 μM and 1500 μM. The figure compares dimer concentrations versus time at 830 μM for ODEs (solid line) and LaBB (solid circles) with dimer concentrations versus time at 1500 μM for ODEs (dashed line) and LaBB (open circles).

introduced by altering the probabilities of protein motion to be vectorally favorable from quadrant IV toward I. The polymerization in a pseudo steady-state is observed to be a gradient with the highest concentration of the actin filaments in quadrant I of the model (Fig. 4B). This is quantified by examining the number of initial monomers that are present in each of four quadrants, which are defined by an equal distributed distance across the vertical axis. Starting from an initial uniform monomer distribution, the concentration rapidly decreases in quadrant IV due to this polarized protein mobility (Fig. 4C). This G-actin concentration differential is partially remediated by the transition from a monomer to filamentous form that is simultaneously occurring. The distribution of the total filament population (a summation of all actin assemblies in non-monomeric form) is initially zero due to the initial conditions of polymer absence (Fig. 4D). The increase in total filaments in quadrant IV is minimal due to the movement of the free monomers toward quadrant I. The increase in the total filaments in quadrant I reaches a final concentration that is multi-fold higher relative to quadrant II-IV. This polarization of actin filament quantities has been observed in the chemotactic cells as cells exhibit a gradient distribution of actin monomers and filaments biased toward the leading edge.

This non-uniform distribution occurs at the leading edge of cells where the height of the cell is minimal, suggesting that a two-dimensional model will accurately describe the system. However a three-dimensional model, although computationally more expensive, could provide more insight into these systems. To address this, we developed an object oriented Java-based model with similar parameters to those used in the two-dimensional environment. The monomers have a higher degree of freedom due to the potential occupancy in 26 adjacent sites versus the 4 used in the two-dimensional model. Further the binding is also increased as there are 26 adjacent binding locations for mobile G-actin. The polymerization and actin mobility is revealed to produce similar protein-filament profiles compared to the relative concentrations of proteins and filaments as observed in the two-dimensional studies (Fig. 5). Fig 5A shows that at relatively low concentrations, ODE and LaBB solutions converge in three dimensional models similarly to two-dimensional models. Comparison between lower and higher concentration polymerization for single species

(Fig. 5B) reveals a sharp divergence between ODE and LaBB at high concentrations that is not seen at lower concentrations. This latter result is again consistent with the two-dimensional results. Under the assumptions of the current model, however, the three-dimensional simulations require a significantly higher concentration to yield an evident effect in comparison to the two-dimensional simulations. This is likely due to the greater difficulty of two polymers interfering with one another through steric hindrance in a three-dimensional space.

The ability to understand the self-assembly of the actin cytoskeleton will allow us to begin to study the link between mechanics and biochemistry through the formation and organization of cell structure that is known to contribute to this mechanosensitive pathway. In these studies, the LaBB model allows us to probe questions in these molecular environments that are relevant in a biological context. While the ODEs capture the overall performance in actin formation, when there is an introduction of non-homogeneity or gradient characteristics, they must be continuously adjusted to capture the system behavior. Molecular distribution and structure in cells is inherently a non-uniform system and thus a more robust system is necessary. Even reaction-diffusion models that explicitly account for spatial gradients will not account for steric hindrance and excluded volume effects. The LaBB system is able to capture the essential behaviors of these polymerization processes with a minimum of additional parameters required. Results with the LaBB model suggest that spatial limitations have significant quantitative effects at physiological concentrations. These results also portend the utility of this system for examining other structurally and spatially constrained systems linked to the actin cytoskeleton, including the FAC and the extracellular matrix. This indicates that exploring cell structure and cytoskeletal assembly can be the genesis for a variety of studies involving cellular and molecular mechanics, transport, and organization.

Acknowledgement: We would like to thank S. LeDuc for helpful discussions. This work was supported in part by the National Science Foundation-CAREER, the Berkman Foundation, and the Pennsylvania Infrastructure Technology Alliance. KP thanks the Merck Computational Biology and Chemistry Program for a doctoral fellowship.

References

Alberts, B.; Bray, A.; Lewis, J.; Raff, M.; Roberts, K.; Watson, J. (1994): "Molecular Biology of the Cell, 3rd. Ed." Garland Publishing, Inc., New York.

Alfa, C. E.; Hyams, J. S. (1990): Distribution of tubulin and actin through the cell division cycle of the fission yeast Schizosaccharomyces japonicus var. versatilis: a comparison with Schizosaccharomyces pombe. *J Cell Sci*, 96 (Pt 1): 71-77.

Chen, L.; Janetopoulos, C.; Huang, Y. E.; Iijima, M.; Borleis, J.; Devreotes, P. N. (2003): Two phases of actin polymerization display different dependencies on PI(3,4,5)P3 accumulation and have unique roles during chemotaxis. *Mol Biol Cell*, 14: 5028-5037.

Ferrer, I.; Blanco, R.; Carmona, M.; Puig, B.; Barrachina, M.; Gomez, C.; Ambrosio, S. (2001): Active, phosphorylation-dependent mitogen-activated protein kinase (MAPK/ERK), stress-activated protein kinase/c-Jun N-terminal kinase (SAPK/JNK), and p38 kinase expression in Parkinson's disease and Dementia with Lewy bodies. *J Neural Transm*, 108: 1383-1396.

Gamble, E.; Koch, C. (1987): The dynamics of free calcium in dendritic spines in response to repetitive synaptic input. *Science*, 236: 1311-1315.

Goodsell, D. S. (1993): "The machinery of life". Springer-Verlag, New York, NY.

Hall, D. (2002): On the role of the macromolecular phase transitions in biology in response to change in solution volume or macromolecular composition: action as an entropy buffer. *Biophys Chem*, 98: 233-248.

Henson, S. M.; Costantino, R. F.; Cushing, J. M.; Desharnais, R. A.; Dennis, B.; King, A. A. (2001): Lattice effects observed in chaotic dynamics of experimental populations. *Science*, 294: 602-605.

Hernandez-Cruz, A.; Sala, F.; Adams, P. R. (1990): Subcellular calcium transients visualized by confocal microscopy in a voltage-clamped vertebrate neuron. *Science*, 247: 858-862.

Hodgson, L.; Qiu, W.; Dong, C.; Henderson, A. J. (2000): Use of green fluorescent protein-conjugated beta-actin as a novel molecular marker for in vitro tumor cell chemotaxis assay. *Biotechnol Prog*, 16: 1106-1114.

Jensen, C.; Hill, C. S. (1994): Mechanical support for congestive heart failure in infants and children. *Crit Care Nurs Clin North Am*, 6: 165-174.

Kiss, E.; Ball, N. A.; Kranias, E. G.; Walsh, R. A. (1995): Differential changes in cardiac phospholamban and sarcoplasmic reticular Ca(2+)-ATPase protein levels. Effects on Ca2+ transport and mechanics in compensated pressure-overload hypertrophy and congestive heart failure. *Circ Res*, 77: 759-764.

LeDuc, P.; Haber, C.; Bao, G.; Wirtz, D. (1999): Dynamics of individual flexible polymers in a shear flow. *Nature*, 399: 564-566.

Levine, E.; Kafri, Y.; Mukamel, D. (2001): Ordering dynamics of the driven lattice-gas model. *Phys Rev E Stat Nonlin Soft Matter Phys*, 64: 026105.

Li, C.; Hu, Y.; Mayr, M.; Xu, Q. (1999): Cyclic strain stress-induced mitogen-activated protein kinase (MAPK) phosphatase 1 expression in vascular smooth muscle cells is regulated by Ras/Rac-MAPK pathways. *J Biol Chem*, 274: 25273-25280.

Marx, J. (2003): How cells step out. *Science*, 302: 214-216.

Meyer, C. J.; Alenghat, F. J.; Rim, P.; Fong, J. H.; Fabry, B.; Ingber, D. E. (2000): Mechanical control of cyclic AMP signalling and gene transcription through integrins. *Nat Cell Biol*, 2: 666-668.

Minton, A. P. (2001): The influence of macromolecular crowding and macromolecular confinement on biochemical reactions in physiological media. *Journal of Biological Chemistry*, 276: 10577-10580.

Moulder, G. L.; Huang, M. M.; Waterston, R. H.; Barstead, R. J. (1996): Talin requires beta-integrin, but not vinculin, for its assembly into focal adhesion-like structures in the nematode Caenorhabditis elegans. *Mol Biol Cell*, 7: 1181-1193.

Puskar, K.; Schwartz, R.; Ta'asan, S.; LeDuc, P. (2004): Spatial Constraints in Polymer Assembly Systems through Coarse Grained Modeling. In submission.

Rao, J. Y.; Hurst, R. E.; Bales, W. D.; Jones, P. L.; Bass, R. A.; Archer, L. T.; Bell, P. B.; Hemstreet, G. P., 3rd (1990): Cellular F-actin levels as a marker for cellular transformation: relationship to cell division and differentiation. *Cancer Res*, 50: 2215-2220.

Resnick, N.; Yahav, H.; Khachigian, L. M.; Collins, T.; Anderson, K. R.; Dewey, F. C.; Gimbrone, M. A., Jr. (1997): Endothelial gene regulation by laminar shear stress. *Adv Exp Med Biol*, 430: 155-164.

Sachs, F. (1991): Mechanical transduction by membrane ion channels: a mini review. *Mol Cell Biochem*, 104: 57-60.

Schaerer-Brodbeck, C.; Riezman, H. (2000): Interdependence of filamentous actin and microtubules for asymmetric cell division. *Biol Chem*, 381: 815-825.

Shabunin, A. V.; Baras, F.; Provata, A. (2002): Oscillatory reactive dynamics on surfaces: a lattice limit cycle model. *Phys Rev E Stat Nonlin Soft Matter Phys*, 66: 036219.

Takeishi, Y. et al. (2001): Src and multiple MAP kinase activation in cardiac hypertrophy and congestive heart failure under chronic pressure-overload: comparison with acute mechanical stretch. *J Mol Cell Cardiol*, 33: 1637-1648.

Tang, D. D.; Wu, M. F.; Opazo Saez, A. M.; Gunst, S. J. (2002): The focal adhesion protein paxillin regulates contraction in canine tracheal smooth muscle. *J Physiol*, 542: 501-513.

Valerius, N. H.; Stendahl, O. I.; Hartwig, J. H.; Stossel, T. P. (1982): Distribution of actin-binding protein and myosin in neutrophils during chemotaxis and phagocytosis. *Adv Exp Med Biol*, 141: 19-28.

Wang, N.; Butler, J. P.; Ingber, D. E. (1993): Mechanotransduction across the cell surface and through the cytoskeleton. *Science*, 260: 1124-1127.

White, S. J.; Jacobs, R. S. (1981): Inhibition of cell division and of microtubule assembly by elatone, a halogenated sesquiterpene. *Mol Pharmacol*, 20: 614-620.

Yamazaki, T.; Komuro, I.; Kudoh, S.; Zou, Y.; Nagai, R.; Aikawa, R.; Uozumi, H.; Yazaki, Y. (1998): Role of ion channels and exchangers in mechanical stretch-induced cardiomyocyte hypertrophy. *Circ Res*, 82: 430-437.